

## Preclinical Development

**Stromal Platelet-Derived Growth Factor Receptor  $\alpha$  (PDGFR $\alpha$ ) Provides a Therapeutic Target Independent of Tumor Cell PDGFR $\alpha$  Expression in Lung Cancer Xenografts**David E. Gerber<sup>1</sup>, Puja Gupta<sup>2</sup>, Michael T. Dellinger<sup>3,4</sup>, Jason E. Toombs<sup>3</sup>, Michael Peyton<sup>4</sup>, Inga Duignan<sup>5</sup>, Jennifer Malaby<sup>5</sup>, Timothy Bailey<sup>5</sup>, Colleen Burns<sup>5</sup>, Rolf A. Brekken<sup>3,4</sup>, and Nick Loizos<sup>5</sup>**Abstract**

In lung cancer, platelet-derived growth factor receptor  $\alpha$  (PDGFR $\alpha$ ) is expressed frequently by tumor-associated stromal cells and by cancer cells in a subset of tumors. We sought to determine the effect of targeting stromal PDGFR $\alpha$  in preclinical lung tumor xenograft models (human tumor, mouse stroma). Effects of anti-human (IMC-3G3) and anti-mouse (1E10) PDGFR $\alpha$  monoclonal antibodies (mAb) on proliferation and PDGFR $\alpha$  signaling were evaluated in lung cancer cell lines and mouse fibroblasts. Therapy studies were conducted using established PDGFR $\alpha$ -positive H1703 cells and PDGFR $\alpha$ -negative Calu-6, H1993, and A549 subcutaneous tumors in immunocompromised mice treated with vehicle, anti-PDGFR $\alpha$  mAbs, chemotherapy, or combination therapy. Tumors were analyzed for growth and levels of growth factors. IMC-3G3 inhibited PDGFR $\alpha$  activation and the growth of H1703 cells *in vitro* and tumor growth *in vivo*, but had no effect on PDGFR $\alpha$ -negative cell lines or mouse fibroblasts. 1E10 inhibited growth and PDGFR $\alpha$  activation of mouse fibroblasts, but had no effect on human cancer cell lines *in vitro*. *In vivo*, 1E10-targeted inhibition of murine PDGFR $\alpha$  reduced tumor growth as single-agent therapy in Calu-6 cells and enhanced the effect of chemotherapy in xenografts derived from A549 cells. We also identified that low expression cancer cell expression of VEGF-A and elevated expression of PDGF-AA were associated with response to stromal PDGFR $\alpha$  targeting. We conclude that stromal PDGFR $\alpha$  inhibition represents a means for enhancing control of lung cancer growth in some cases, independent of tumor cell PDGFR $\alpha$  expression. *Mol Cancer Ther*; 11(11); 2473–82. ©2012 AACR.

**Introduction**

Platelet-derived growth factor receptor (PDGFR) is a transmembrane receptor tyrosine kinase. Upon binding

of circulating PDGF ligand, PDGFR $\alpha$  and  $\beta$  subunits homodimerize or heterodimerize, undergo autophosphorylation, and activate downstream signal transduction molecules including phosphoinositide 3-kinase, Ras, phospholipase C- $\gamma$ , Src, and signal transducer and activator of transcription (1). In normal physiology, PDGFR $\alpha$  functions in early and late stages of embryonic development (during which it drives proliferation of undifferentiated mesenchymal populations, tissue remodeling, and cellular differentiation), wound healing, angiogenesis, and modulating interstitial fluid pressure (2, 3).

When expressed on cancer cells, PDGFR $\alpha$  has been implicated in the development and progression of several malignancies (4). Co-expression of PDGF and PDGFR $\alpha$  has been reported in various cancer types, consistent with autocrine-mediated growth (3). In lung cancer, expression of PDGF and/or PDGFR $\alpha$  is associated with more aggressive tumor biology and worse prognosis (5). Specific genetic alterations of the PDGF-PDGFR $\alpha$  axis occur in gastrointestinal stromal tumors (activating mutations in the intracellular domain of PDGFR $\alpha$ ; ref. 6), certain gliomas and NSCLCs (PDGFR $\alpha$  amplification; refs. 7, 8), dermatofibrosarcoma protuberans (a 17;22 chromosomal translocation resulting in a fusion oncogene encoding PDGF-B; ref. 9), and hypereosinophilic syndrome (*FIP1L1-PDGFR $\alpha$*  fusion transcripts; ref. 10).

**Authors' Affiliations:** Divisions of <sup>1</sup>Hematology-Oncology, <sup>2</sup>Pediatric Hematology-Oncology, <sup>3</sup>Surgical Oncology, and the <sup>4</sup>Hamon Center for Therapeutic Oncology Research, Harold C. Simmons Cancer Center, University of Texas Southwestern Medical Center, Dallas, Texas; <sup>5</sup>ImClone Systems, New York, New York

**Note:** Supplementary data for this article are available at Molecular Cancer Therapeutics Online (<http://mct.aacrjournals.org/>).

Presented in part at the Cancer Prevention and Research Institute of Texas (CPRIIT) Innovations in Cancer Prevention and Research Conference, Austin, Texas, November 17–29, 2010 and at the 47<sup>th</sup> annual meeting of the American Society of Clinical Oncology, Chicago, Illinois, June 3–7, 2011.

Current address for P. Gupta: Arizona Cancer Center, University of Arizona Medical Center, Tucson, AZ.

**Corresponding Authors:** David E. Gerber, Harold C. Simmons Cancer Center, University of Texas Southwestern Medical Center, 5323 Harry Hines Blvd, Mail Code 8852, Dallas, TX 75390-8852. Phone: 214-648-4180; Fax: 214-648-1955; E-mail: david.gerber@utsouthwestern.edu; and Nick Loizos, Department of Cell Biology, ImClone Systems, a wholly owned subsidiary of Eli Lilly and Company, Alexandria Center for Life Sciences, 450 East 29<sup>th</sup> Street, 12<sup>th</sup> Floor, New York, NY 10016. Phone: 646-638-5015; Fax: 212-645-2054; E-mail: Nick.Loizos@lmclone.com

doi: 10.1158/1535-7163.MCT-12-0431

©2012 American Association for Cancer Research.

Given the encouraging results achieved with targeting epidermal growth factor receptor (EGFR) and anaplastic lymphoma kinase (ALK) in patients with lung tumors harboring *EGFR* mutations and *ALK* translocations, recent PDGFR $\alpha$  research has focused on identifying those lung cancers with aberrant tumor cell PDGFR $\alpha$  activity as potential candidates for PDGFR $\alpha$ -directed therapy. For instance, in a recent screen of NSCLC cell lines, 1 of 103 cell lines responded *in vitro* to the PDGFR inhibitor sunitinib (11). The sensitive cell line, H1703, was noted to have high-level *PDGFRA* amplification. Among the larger set of 637 human tumor-derived cell lines evaluated in the study, only one other, the PDGFR $\alpha$ -positive A-204 rhabdomyosarcoma cell line, responded to sunitinib, suggesting that only rare solid tumor patients might benefit from PDGFR $\alpha$  inhibition. However, such an approach does not account for the potential therapeutic effects of stromal PDGFR $\alpha$  inhibition. In tumor stroma, the PDGF-PDGFR $\alpha$  axis functions in fibroblast activation, aberrant epithelial-stromal interactions, modulation of tumor interstitial pressure, and production and secretion of VEGF (12–14). In studies with VEGF-null tumorigenic cells, PDGF-AA was identified as the major stromal fibroblast chemotactic factor produced by the tumor cells that lead to recruitment of VEGF-producing stromal fibroblasts for tumor angiogenesis and growth (14).

To determine the effects of stromal PDGFR $\alpha$  inhibition, we capitalized on xenograft modeling of cancer (human tumor cells, mouse stromal cells) and the availability of species-specific anti-PDGFR $\alpha$  monoclonal antibodies (mAbs). In this model, IMC-3G3, a fully human anti-human PDGFR $\alpha$  mAb, targets tumor cell PDGFR $\alpha$  (15), whereas 1E10, a fully human anti-mouse PDGFR $\alpha$  mAb, targets stromal PDGFR $\alpha$ . Our studies show that targeting stromal PDGFR $\alpha$  has single-agent antitumor activity and the potential to enhance the effect of chemotherapy in murine models of lung cancer. The cell lines of xenografts sensitive to targeting stromal PDGFR $\alpha$  expressed a high PDGF-AA/VEGF-A ratio relative to a resistant xenograft line, thus suggesting a potential selection strategy for therapy.

## Materials and Methods

### Cell culture

With the exception of A549, which was purchased from the American Type Culture Collection (ATCC), all tumor cell lines were provided by Dr. John Minna (UT Southwestern, Dallas, TX; ref. 16). Cell lines were authenticated. Specifically, the identity of each cell line was confirmed by DNA fingerprinting via short tandem repeats using the PowerPlex 1.2 kit (Promega). Fingerprinting results were compared with reference fingerprints. All cancer cell lines were grown in a humidified atmosphere with 5% CO<sub>2</sub> at 37°C in RPMI-1640 medium (Life Technologies Inc.) supplemented with 5% FBS. Each cell line was DNA fingerprinted for provenance using the PowerPlex 1.2 kit (Promega) and confirmed to be the same as

the DNA fingerprint library maintained by ATCC and the Minna/Gazdar lab (the primary source of the lines), and confirmed to be free of mycoplasma by e-Myco kit (Boca Scientific).

Using previously generated genomic microarray data (Affymetrix, Inc. and Illumina, Inc.), 29 NSCLC cell lines with varying expression of PDGFR $\alpha$  were identified. To confirm microarray findings, selected cells were grown in media, harvested at 70% to 80% confluency, and lysates extracted. Equal amounts of protein were subjected to SDS-PAGE followed by Western blot analysis with anti-PDGFR $\alpha$  antibodies and detected by chemiluminescence. In addition, confirmation by quantitative PCR was carried out. RNA was prepared using TRIzol (Invitrogen) according to the manufacturer's instructions. The quality of RNA was evaluated using spectrophotometry. The cDNA used for subsequent PCR was made using iScript (Bio-Rad Laboratories). The expression of *human PDGFR $\alpha$*  was analyzed by quantitative real-time RT-PCR using an assay on demand (Mm00440111\_m1) from Applied Biosystems. Mouse *GAPDH* and human *RPLPO* (Applied Biosystems assay-on-demand) were used as internal reference genes to normalize input cDNA. Quantitative real-time RT-PCR was carried out in a reaction volume of 25  $\mu$ L including 5  $\mu$ L of cDNA, and each reaction was done in triplicate. The comparative Ct method was used to compute relative expression values (17).

### Anti-PDGFR $\alpha$ antibody generation and characterization

Anti-mouse PDGFR $\alpha$  antibody 1E10 was obtained by selection of a human naïve display Fab library (18) on recombinant mouse PDGFR $\alpha$  extracellular domain protein following a protocol described previously (19). After being converted into full-length IgG format, 1E10 was expressed in NS0 cells as described (20). Full-length IgG1 antibody was purified by protein A affinity chromatography (Poros A, PerSeptive Biosystems, Inc.). IMC-3G3, a fully human anti-human PDGFR $\alpha$  IgG1 mAb, was developed as reported previously (15).

Antibody species specificity was confirmed in a solid-phase blocking assay and cell-based signaling assays. In the solid-phase blocking assay, antibodies were first mixed with a fixed amount of mouse PDGFR $\alpha$ /Fc (50 ng at 0.5  $\mu$ g/mL, R&D Systems). The mixture was transferred to 96-well plates precoated with PDGF-AA (100 ng/well), followed by incubation with a goat anti-human Fc antibody-HRP conjugate (Jackson ImmunoResearch). Plates were read at A<sub>450</sub> nm using a microplate reader (Molecular Devices).

### Growth factor quantitation

Cells were seeded into 100 mm tissue culture dishes and maintained in 15 mL of media for 96 hours at 5% CO<sub>2</sub> and 37°C. At the 96-hour time point, cell monolayers were approximately 85% to 90% confluent. The media was collected and spun 3 times at 1,000  $\times$  g to remove particulate matter. The concentration of PDGF-AA and VEGF-A

in the media was measured by ELISA (Quantikine kits from R&D systems; cat. # DAA00B and DVE00). The cells in the dishes were washed with PBS, removed by trypsin and counted for normalization of growth factor concentration to cell number.

### Cell-signaling assays

Receptor and downstream signaling molecule phosphorylation assays were carried out as described (15). Cell lysates were prepared in lysis buffer a (150 mmol/L NaCl, 50 mmol/L Tris pH 7.4, 1% Triton X-100, 1 mmol/L EDTA, 10 mmol/L NaPP<sub>i</sub>, 50 mmol/L NaF, 1 mmol/L Na<sub>3</sub>VO<sub>4</sub>) with protease inhibitors (Roche, cat. no. 04 693 124 001) and PhosSTOP phosphatase inhibitor (Roche, cat. no. 04 906 845 001). Lysates were separated by SDS-PAGE and transferred to PVDF membranes. Membranes were probed with the following antibodies: anti-PDGFR $\alpha$  (Cell Signaling Technology, #3174), anti-PDGFR $\alpha$  (Neomarkers, RB-9027), phospho-PDGFR $\alpha$  (Santa Cruz Biotechnology, sc-12910), anti- $\beta$ -actin (Santa Cruz, sc-8432), anti-phospho-PLC $\gamma$  (Cell Signaling Technology, #2821), anti-PARP (Cell Signaling, #9542), and anti-PDGF-C (Santa Cruz Biotechnology, sc-18228). Antibody reactivity was detected using the appropriate peroxidase conjugated secondary antibody (Jackson ImmunoResearch) and subsequent chemiluminescence substrate (Pierce).

### MTS assay

Assays were carried out as described previously (21). In brief, 500 to 4,000 cells were allowed to seed for 24 hours before 4-fold serial dilutions of drug were added. The maximum dose was 500  $\mu$ g/mL ( $\sim$ 3,300 nmol/L) for IMC-3G3 and 1E10. Cells were incubated for 4 days then relative cell number was determined by the addition of MTS (Promega, final concentration 333  $\mu$ g/mL), incubating for 1 to 3 hours at 37°C and reading absorbance at 490 nm in a plate reader (Spectra Max 190, Molecular Devices). Each experiment contained 8 replicates per concentration and the entire assay was carried out in multiple replicates. Drug sensitivity curves and IC<sub>50</sub> values were calculated using in-house software (DIVISA).

### Animal studies

Animal studies were conducted according to U.S. Department of Agriculture and NIH guidelines and approved by the respective Institutional Animal Care and Use Committees. Female athymic nude (CrI:NU/NU-nuBR, Charles River Laboratories) or SCID mice were implanted subcutaneously with 5 to 20  $\times$  10<sup>6</sup> cells from selected NSCLC cell lines, as previously described (15). For the H1703 monotherapy study, mice were randomized into 2 groups ( $n = 12$ ) and treated with human IgG (40 mg/kg) or IMC-3G3 (40 mg/kg) 3 times weekly. There is a precedent in animal studies for antibody treatment at 40 mg/kg to achieve circulating antibody trough levels consistent with those achieved in man. For example, the target serum concentration for IMC-3G3 is hypothesized to be one that maintains con-

centrations above levels associated with inhibition of the growth of human tumor growth xenograft models in mice (155 to 258  $\mu$ g/mL). Results of the PK data from patients in the IMC-3G3 phase 1 study show that IMC-3G3 dosing yielded serum concentrations at or above the target trough concentrations (22).

In the 1E10 plus chemotherapy combination studies in A549 and H1993 xenografts, cohorts of animals with established tumors were randomized into 4 groups ( $n = 8$ ) and treated with (1) vehicle, (2) chemotherapy (cisplatin, 1 mg/kg 1 $\times$ /week; gemcitabine 25 mg/kg, 2 $\times$ /week), (3) 1E10, or (4) chemotherapy plus 1E10. Mice were treated by i.p. injection twice weekly for the duration of the study. In each group, on the day of dosing, the first treatment listed above was administered first, followed by the second treatment 30 minutes later. Tumor volumes were evaluated twice weekly. In all xenograft studies, animals were assessed for toxicity (weight loss, death, cage side observations) and tumors were measured twice weekly. Tumor volume was calculated according to the formula  $\pi/6 \times$  longest length  $\times$  perpendicular width<sup>2</sup>. Tumor growth in the treatment groups was compared with a repeated-measures ANOVA.

Tumors were harvested for analysis of growth factors by ELISA and Western blotting. Tumors were homogenized in lysis buffer b (Cell Signaling, cat. no. 9803) supplemented with protease inhibitors (Roche) and Phos-Stop phosphatase inhibitor (Roche). The lysates were centrifuged twice at 14,000 rpm and the protein concentration for the collected supernatant was determined (Bio-Rad, cat. no. 500-0116).

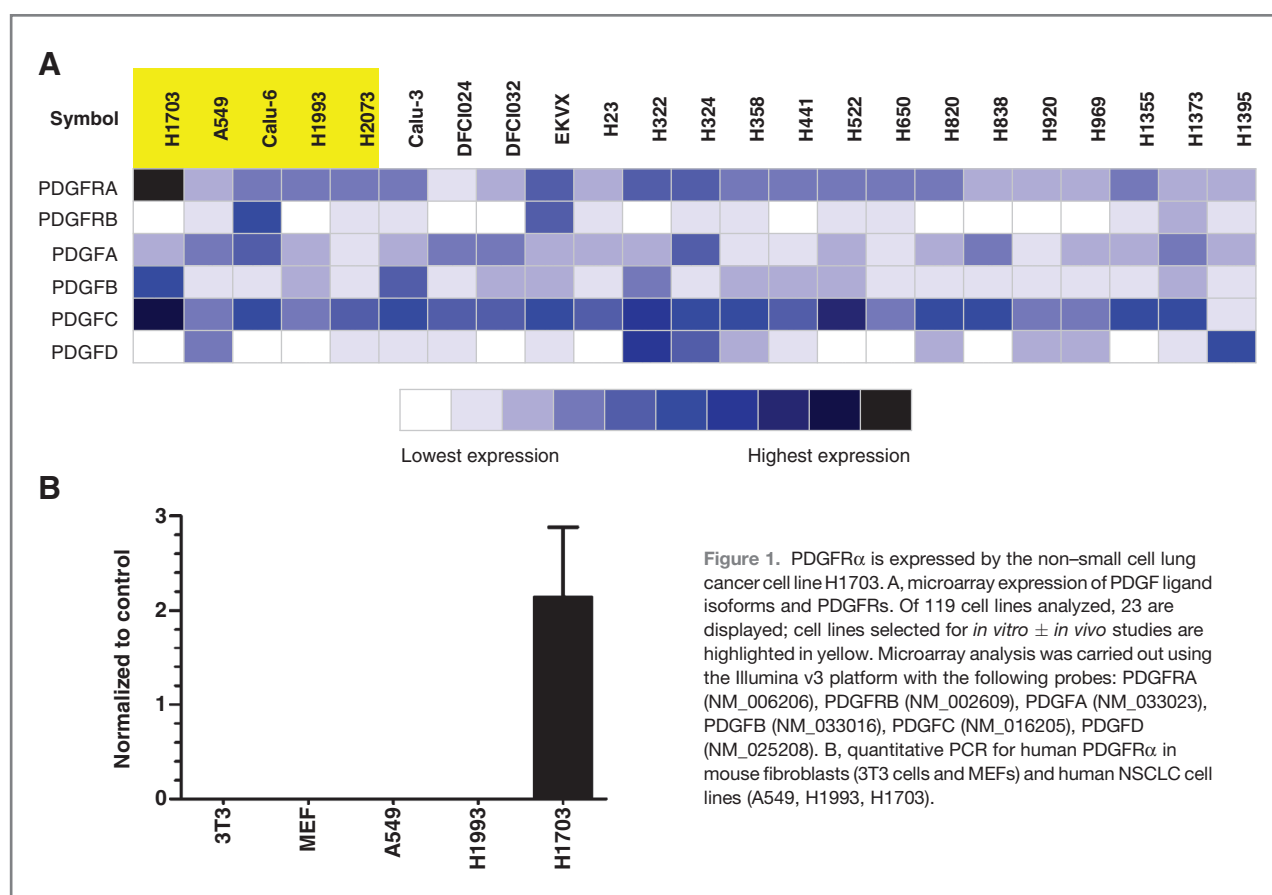
### Statistical analysis

For cell proliferation assays, sigmoidal dose response curves were fitted and the inhibitory concentrations at 50% (IC<sub>50</sub>) were calculated using the Weibull model. Tumor volumes and weights were compared using the Student *t* test. For IHC studies, tumors were analyzed and compared by one-way ANOVA, followed by Fisher LSD Post hoc test for multiple comparisons. The number of samples in each group was always taken as the number of tissues used in the analysis. For PDGF-CC analysis, Adobe Photoshop 7 was used to determine the mean luminosity of the Western blotting protein bands. The mean luminosity of each PDGF-C GFD band was normalized by the mean luminosity of the respective  $\beta$ -actin band. These values were plotted in GraphPad Prism 5, and an unpaired *t* test was used to determine significance. All calculated *P* values are 2 sided. For all tests, *P* < 0.05 was considered significant.

## Results

### NSCLC cell line PDGFR $\alpha$ expression and response to inhibition

PDGFR $\alpha$  expression was evaluated by microarray analysis in a panel of NSCLC cell lines ( $n = 119$ ; Fig. 1a). A subset of these lines ( $n = 32$ ) were screened



for protein expression by Western blot analysis (Supplementary Fig. S1). PDGFR $\alpha$  expression was shown in human H1703 NSCLC cells, but not in A549 or H1993 cells or in mouse fibroblasts (3T3 cells and MEFs; Fig. 1b). Twenty-nine NSCLC cell lines with varying PDGFR $\alpha$  expression by microarray analysis were selected and treated *in vitro* with escalating concentrations of IMC-3G3. A single cell line, H1703, expressed PDGFR $\alpha$  robustly at the protein level and showed sensitivity to IMC-3G3 with an IC<sub>50</sub> of 225 nmol/L (34  $\mu$ g/mL). All other cell lines (including A549, H1993, and Calu-6) showed resistance to IMC-3G3, with IC<sub>50</sub> greater than 3,300 nmol/L (500  $\mu$ g/mL; see Table 1). The PDGFR $\alpha$ -positive H1703 lung cancer line contains both PDGFR $\alpha$  and PDGF-CC gene amplifications and shows a codependency on this axis for proliferation (11). Codependence of this kind is a rare event in human lung cancer cell lines, suggesting that only a limited number of lung tumor patients might benefit from tumor cell PDGFR $\alpha$  inhibition. In contrast, IMC-3G3 did not inhibit proliferation of H1792 cells (IC<sub>50</sub> > 500  $\mu$ g/mL). These cells overexpress PDGFR $\alpha$  (see Supplementary Fig. S1) but not PDGF ligand (11). This observation suggests that, in the absence of PDGFR $\alpha$  mutation or amplification, overexpression of both ligand and receptor are required for cell autonomous growth.

### Characterization of IMC-3G3 and 1E10

We capitalized on the xenograft model (human cancer cells, mouse stromal cells) and species-specific mAbs to evaluate the effects of inhibiting tumor cell and stromal PDGFR $\alpha$ . Species-specific targeting was showed through binding assays, Western blot analysis, and effects on receptor activation and signaling. The anti-human PDGFR $\alpha$  mAb IMC-3G3 has been previously described (15). To target stromal PDGFR $\alpha$ , an anti-mouse PDGFR $\alpha$  mAb (1E10) was generated. 1E10 was shown to inhibit PDGF-AA from binding to murine PDGFR $\alpha$  with an IC<sub>50</sub> of  $8.51 \times 10^{-9}$  M (Fig. 2a). IMC-3G3 had no blocking effect in this assay. Antibody 1E10 showed immunoreactivity with PDGFR $\alpha$ -positive mouse fibroblasts but not with PDGFR $\alpha$ -positive human H1703 NSCLC cells (Supplementary Fig. S2). Conversely, IMC-3G3 had immunoreactivity with PDGFR $\alpha$ -positive human H1703 NSCLC cells but not with PDGFR $\alpha$ -positive mouse fibroblasts or with PDGFR $\alpha$ -negative human A549 NSCLC cells (Supplementary Fig. S2). Therefore, the use of IMC-3G3 in subcutaneous human xenograft models using tumors lines that are PDGFR $\alpha$ -negative would be ineffective and would not discern the therapeutic effects of stromal PDGFR $\alpha$  inhibition. PDGF-AA-mediated phosphorylation of PDGFR $\alpha$  and PLC $\gamma$  in H1703 cells was inhibited by IMC-3G3 but

**Table 1.** Expression of PDGF-AA and VEGF-A and response to PDGFR $\alpha$  inhibition in lung cancer cell lines grown in culture and *in vivo*

Cell line	Avg PDGF-AA (ng/mL/10 <sup>5</sup> cells $\pm$ SD)	Avg VEGF-A (ng/mL/10 <sup>5</sup> cells $\pm$ SD)	Ratio PDGF-AA/ VEGF-A	Ratio VEGF-A/ PDGF AA	<i>In vitro</i> anti- human PDGFR $\alpha$ mAb IC <sub>50</sub> ( $\mu$ g/mL) <sup>a</sup>	<i>In vivo</i> anti-mouse PDGFR $\alpha$ mAb tumor/control volume
Calu-6	0.0708 $\pm$ 0.0350	0.1388 $\pm$ 0.0769	0.510	1.960	>500	0.51
A549	0.07833 $\pm$ 0.0232	0.8518 $\pm$ 0.255	0.092	10.874	>500	0.66
H1993	0.0235 $\pm$ 0.0148 <sup>b</sup>	1.5476 $\pm$ 0.178	0.015	65.855	>500	1.21
H2073	0.0086 $\pm$ 0.0010 <sup>b</sup>	0.5224 $\pm$ 0.131	0.016	60.742	>500	N/A
H1703	Bld	2.0254 $\pm$ 0.0784	N/A	N/A	34	N/A

NOTE: Cells were grown for 96 hours at 37°C and 5% CO<sub>2</sub>. Supernatants were collected and analyzed by ELISAs to quantitate secreted VEGF-A and PDGF-AA.

Abbreviations: Bld, below limits of detection; N/A, not applicable; SD, standard deviation.

<sup>a</sup>With the exception of H1703, all tested NSCLC cell lines (*N* = 29) were resistant to anti-PDGFR $\alpha$  antibody therapy *in vitro* (IC<sub>50</sub> > 500  $\mu$ g/mL).

<sup>b</sup>Extrapolated values.

not by 1E10 (Fig. 2b). In contrast, 1E10 but not IMC-3G3 inhibited activation of PDGFR $\alpha$  and the signal transduction mediator PLC $\gamma$  in PDGF-stimulated mouse fibro-

blasts *in vitro* (Fig. 2c). 1E10 inhibited PDGF-AA-induced phosphorylation of mouse PDGFR $\alpha$  but not PDGF-BB-induced phosphorylation of mouse PDGFR $\beta$  (Fig. 2d).

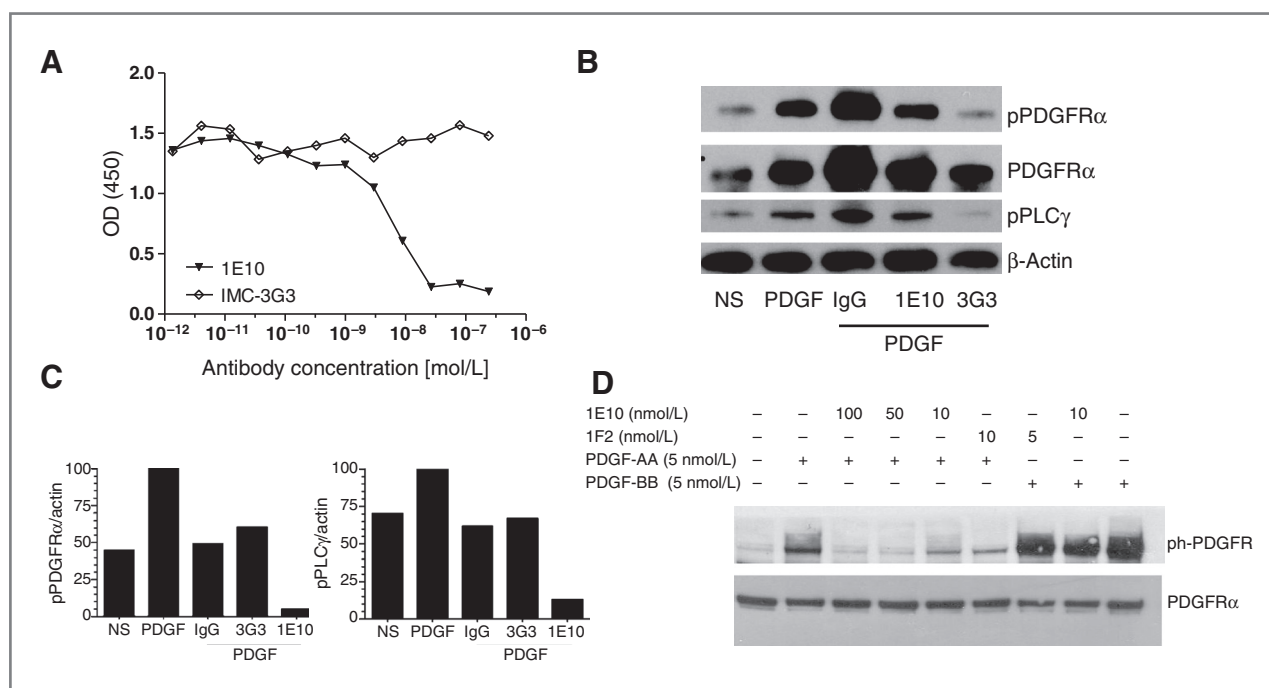


**Figure 2.** Species-specific activity of IMC-3G3 and 1E10. **A**, inhibition of mouse PDGFR $\alpha$  binding to immobilized PDGF-AA by 1E10 but not IMC-3G3. Antibodies were preincubated with a fixed amount of Fc-tagged-mouse PDGFR $\alpha$  and then this mixture was transferred to a plate precoated with PDGF-AA. Plate-bound mouse PDGFR $\alpha$  was detected with a goat-anti-human Fc antibody-HRP conjugate. **B**, PDGF-AA-mediated phosphorylation of PDGFR $\alpha$  and PLC $\gamma$  in H1703 cells is inhibited by IMC-3G3 but not by 1E10. H1703 cells were nonstimulated (NS) or stimulated with PDGF-AA 50 ng/mL (1.7 nmol/L) for 5 minutes and treated with antibodies. 1E10 and IMC-3G3 were used at concentrations of 132  $\mu$ g/mL (880 nmol/L). Lysates were prepared 10 minutes after incubation and probed by Western blotting for the targets indicated. **C**, *in vitro* activity of 1E10 in mouse fibroblasts. PDGF-AA-mediated phosphorylation of PDGFR $\alpha$  and PLC $\gamma$  in mouse fibroblasts is inhibited by IMC-3G3 but not by 1E10. Mouse fibroblasts were nonstimulated (NS) or stimulated with PDGF-AA and treated with antibodies. Lysates were prepared 10 minutes after incubation and probed by Western blotting for the targets indicated. **D**, specific inhibition of mouse PDGFR $\alpha$  phosphorylation by 1E10. NIH3T3 mouse fibroblasts were rendered quiescent, treated with mAbs, and then stimulated with either PDGF-AA or PDGF-BB. Afterward, cell lysates were analyzed by SDS-PAGE and Western blotting with an antiphosphotyrosine antibody. 1E10 inhibited PDGF-AA-induced phosphorylation of PDGFR $\alpha$  but not PDGF-BB-induced phosphorylation of PDGFR $\beta$ .

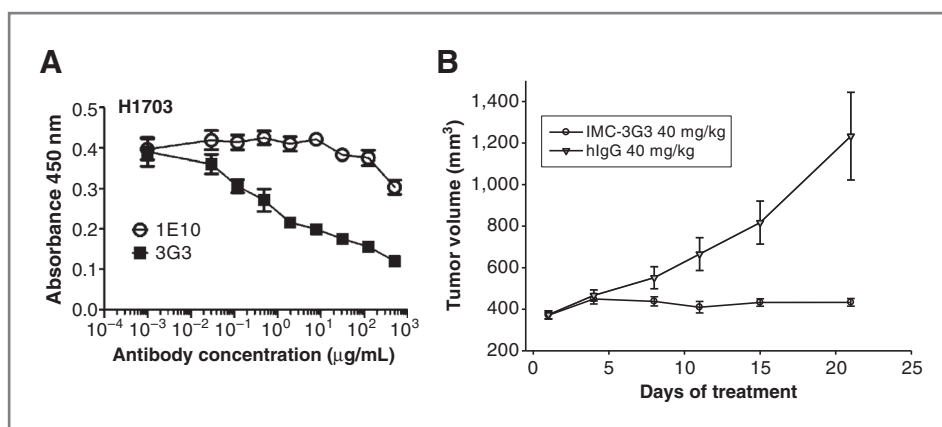


**Figure 3.** *In vitro* and *in vivo* activity of IMC-3G3. A, proliferation of human H1703 cells *in vitro* is inhibited by anti-human PDGFR $\alpha$  monoclonal antibody IMC-3G3 but not by anti-mouse PDGFR $\alpha$  monoclonal antibody 1E10. Cells were allowed to seed for 24 hours before serial dilutions of drug were added. Cells were incubated for 4 days then relative cell number was determined by MTS assay. B, growth inhibition of H1703 tumor xenografts in nude mice treated with 40 mg/kg of IMC-3G3 on a 3 times per week schedule.

### ***In vitro* and *in vivo* activity of IMC-3G3 on PDGFR $\alpha$ -positive NSCLC**

*In vitro*, human H1703 cells were sensitive to IMC-3G3 in MTS assay ( $\text{IC}_{50} = 10 \mu\text{g/mL}$ ), but were resistant to 1E10 ( $\text{IC}_{50} > 1,000 \mu\text{g/mL}$ ; Fig. 3a). In addition, IMC-3G3 significantly inhibited growth of H1703 xenografts ( $P = 0.0003$ , Fig. 3b). Tumors in mice receiving IMC-3G3 (mean final volume  $433 \pm 18 \text{ mm}^3$ ) were significantly smaller than in mice receiving control IgG (mean final volume  $1,233 \pm 211 \text{ mm}^3$ ), corresponding to a 65% reduction in final tumor volume.

### ***In vivo* antitumor activity of 1E10 on PDGFR $\alpha$ -negative xenografts with high PDGF-AA/VEGF-A ratio**

Given that PDGF-AA has been identified as a major stromal fibroblast chemotactic factor produced by tumor cells (14), it may be assumed that xenograft lines that express high PDGF-AA would have a greater dependence on stromal activation for growth. Therefore, 13 lung cancer cell lines were screened for PDGF-AA expression to identify lines for *in vivo* antitumor studies targeting stromal PDGFR $\alpha$ . Specifically, the cell lines were grown *in vitro* and expressed PDGF-AA was measured from the supernatants (Table 1). Two lines expressing the highest PDGF-AA were chosen for *in vivo* therapeutic studies of 1E10. In A549 and Calu-6 xenografts, 1E10 treatment attenuated tumor growth, showing a significant therapeutic effect of stromal targeting (Fig. 4). In Calu-6 xenografts, average tumor size on Day 32 was  $1,273 \pm 187 \text{ mm}^3$  with 1E10 treatment, compared with  $2,483 \pm 302 \text{ mm}^3$  with control IgG ( $P = 0.002$ ; Fig. 4a). In A549 xenografts, average tumor size on Day 36 was  $632 \pm 65 \text{ mm}^3$  with 1E10 treatment, compared with  $960 \pm 93 \text{ mm}^3$  with control IgG ( $P = 0.01$ ; Fig. 4b). 1E10 also enhanced the effect of cisplatin-gemcitabine chemotherapy in A549 xenografts (Fig. 4c). Final tumor weights were as follows: control IgG  $1.05 \pm 0.20 \text{ g}$ , 1E10  $0.74 \pm 0.08 \text{ g}$ , cisplatin-gemcitabine  $0.91 \pm 0.15 \text{ g}$ , cisplatin-gemcitabine plus 1E10  $0.56 \pm 0.05 \text{ g}$  ( $P = 0.04$  for cisplatin-gemcitabine plus 1E10 compared with cisplatin-gemcitabine). Of note, these sensitive cell lines

had relatively low *in vitro* expression of VEGF-A compared with PDGF-AA (VEGF-A/PDGF-AA ratio 1.96 in Calu-6 cells and 10.87 in A549 cells; Table 1).

Targeting of stromal PDGFR $\alpha$  with 1E10 had no activity as a monotherapy on the H1993 xenograft (Fig. 4d). In addition, 1E10 did not enhance the effect of cisplatin-gemcitabine chemotherapy in H1993 xenografts (final weights: control IgG  $0.79 \pm 0.09 \text{ g}$ , 1E10  $0.78 \pm 0.06 \text{ g}$ , cisplatin-gemcitabine  $0.28 \pm 0.05 \text{ g}$ , cisplatin-gemcitabine plus 1E10  $0.26 \pm 0.07 \text{ g}$ ; Fig. 4d). This cell line resistant to stromal PDGFR $\alpha$  inhibition had an elevated VEGF-A/PDGF-AA ratio of 65.86 (Table 1). Also of note, in the H1993 xenografts, chemotherapy alone inhibited tumor growth, but A549 xenografts were resistant to the same regimen.

### **Discussion**

High-throughput *in vitro* screens offer a means to test antitumor agents against multiple cancer cell lines relatively quickly and inexpensively. Although such features have rendered this a preferred approach to early-stage preclinical drug development, these studies provide no insight into tumor stromal effects. For inhibitors of PDGFR $\alpha$ , a target expressed on cancer cells and stromal fibroblasts, *in vivo* testing would facilitate showing the full spectrum of therapeutic effects. In agreement with previous studies (11), this report shows that, *in vitro*, PDGFR $\alpha$ -directed therapy has efficacy in a small proportion of cell lines with PDGFR $\alpha$  overexpression.

However, in addition, stromal PDGFR $\alpha$  targeting *in vivo* reduced tumor growth and enhanced the effect of cytotoxic chemotherapy for 2 xenografts, independent of tumor cell PDGFR $\alpha$  expression. The results are consistent with paracrine effects of the PDGF-PDGFR $\alpha$  axis, in which stromal fibroblasts express PDGFR $\alpha$  and malignant cells secrete PDGFs (23, 24). These results echo those of earlier reports suggesting that therapeutic stromal effects, which become apparent in animal models, might otherwise go unrecognized in cell culture assays (25, 26).

Potential explanations for the therapeutic outcome of stromal-PDGFR targeting include effects on fibroblast

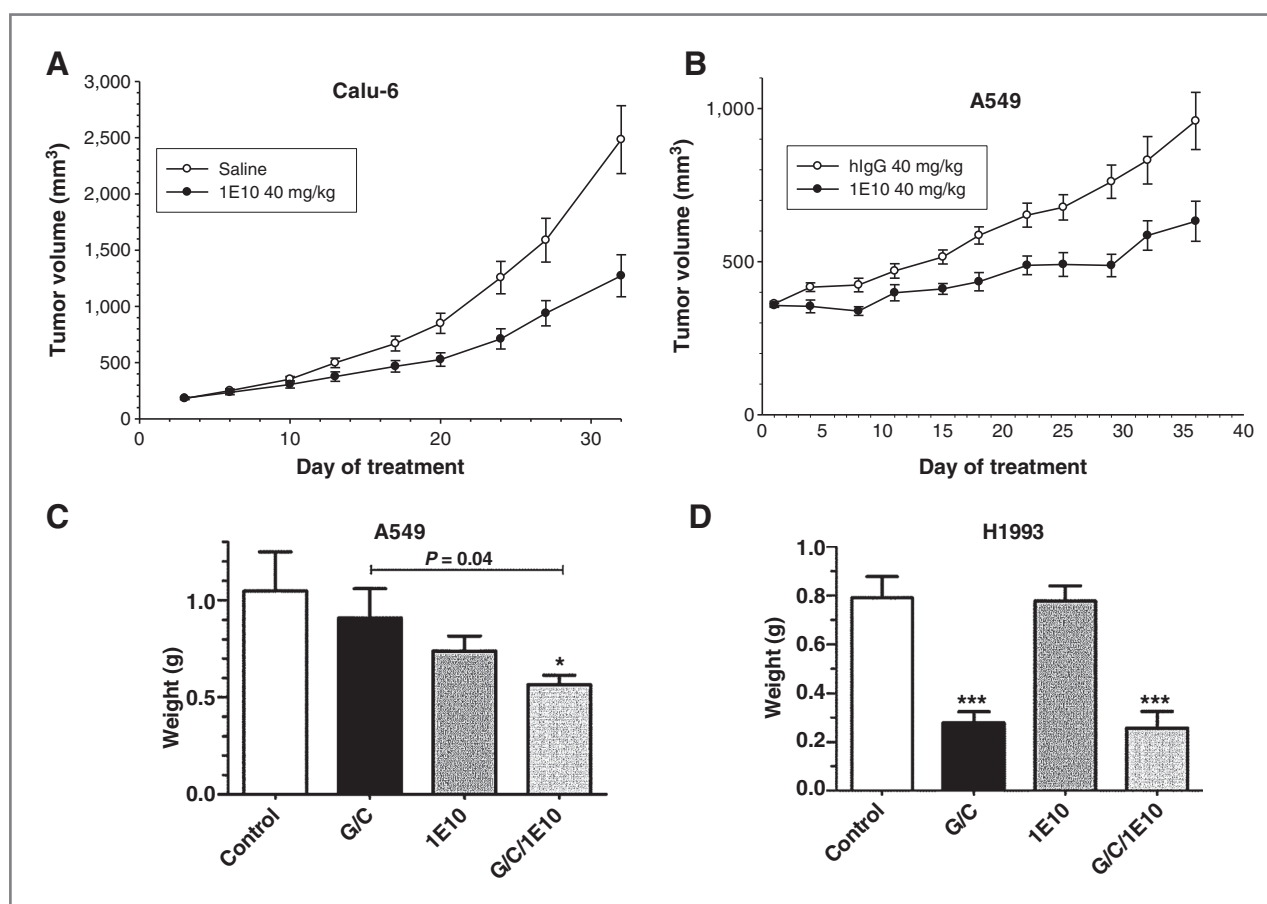


**Figure 4.** *In vivo* activity of 1E10. A, 1E10 inhibited Calu-6 xenograft tumor growth with a T/C value of 51%. This effect was statistically significant ( $P = 0.002$ ). B, 1E10 inhibited A549 xenograft tumor growth with a T/C% of 67%. This effect was statistically significant ( $P = 0.01$ ). C and D, *in vivo* activity of 1E10 in combination with chemotherapy. Tumor-bearing mice were treated with chemotherapy (cisplatin, 1 mg/kg 1 $\times$ /week; gemcitabine 25 mg/kg 2 $\times$ /week), 1E10 twice weekly, or the combination for 3 weeks. C, 1E10 enhanced the antitumor activity of chemotherapy in A549 NSCLC xenografts. D, 1E10 did not enhance the antitumor activity of chemotherapy in H1993 NSCLC xenografts.

activation and angiogenesis (12, 14, 27). In a previous report, PDGF-AA, which binds PDGFR $\alpha$  but not PDGFR $\beta$ , was shown to be the major stromal fibroblast chemotactic factor produced by VEGF-null tumorigenic cells (14). In that system it was concluded that PDGFR $\alpha$  signaling is required for the recruitment of VEGF-producing stromal fibroblasts for tumor angiogenesis and growth. In the present study, tumor cell PDGF-AA and VEGF expression levels suggested an explanation as to why only certain lines responded to stromal PDGFR $\alpha$  inhibition. Elevated cancer cell expression of PDGF-AA and low expression of VEGF were associated with response to stromal PDGFR $\alpha$  targeting. Specifically, sensitive cell lines had relatively low VEGF-A expression (VEGF-A/PDGF-AA ratio 1.96 in Calu-6 cells and 10.87 in A549 cells), whereas the resistant cell line H1993 had elevated VEGF-A (VEGF-A/PDGF-AA ratio 65.86) when grown in cell culture. This difference may suggest that the 1E10-sensitive tumors have a relatively greater dependence on PDGF-AA-induced production of stromal VEGF. Notably, we have previously showed the converse for anti-VEGF monoclonal antibody (bevacizumab) sen-

sitivity, with H1993 xenografts responding to therapy but A549 and Calu-6 exhibiting a poor response (28). If the predictive value of PDGF-AA/VEGF ratio is confirmed preclinically, it would be reasonable to test this biomarker in the clinical setting.

Potential explanations for the effects of stromal PDGFR targeting include effects on angiogenesis, fibroblast activation, and tumor interstitial pressure (12). Preclinical studies have showed that imatinib, a multitargeted tyrosine kinase inhibitor that inhibits PDGFR, reduces interstitial fluid pressure and increases intratumoral concentration of concurrently administered cytotoxic chemotherapy (29, 30). That 1E10 significantly improved the effect of cisplatin-gemcitabine in the A549 xenografts might suggest reduction of tumor interstitial pressure and enhanced chemotherapy delivery. PDGF-activated stromal fibroblasts synthesize collagen, express matrix metalloproteinases, and form a connective tissue network, all of which promote tumor development (31–33). Although the present experiments do not elucidate a therapeutic mechanism of stromal PDGFR $\alpha$  inhibition, it is unlikely that the observed *in vivo* effects represent a nonstromal mechanism. The possibility

that PDGFR $\alpha$ -negative cell lines adapt to express PDGFR $\alpha$  *in vivo* was considered. However, no human PDGFR $\alpha$  was detected in tumor lysates, and the anti-human PDGFR $\alpha$  antibody IMC-3G3 had no effect on A549 xenograft tumor growth (data not shown).

Although a number of PDGFR inhibitors are currently FDA-approved for cancer treatment, these drugs are all relatively nonspecific small molecule kinase inhibitors. This lack of specificity has therapeutic as well as experimental consequences. For instance, due to cross-reactivity with c-KIT, imatinib is associated with hematologic toxicity precluding its concomitant administration with cytotoxic chemotherapy (12). PDGFR kinase inhibitors also inhibit both PDGFR subunits. Inhibition of PDGFR $\beta$ , which is expressed predominantly on vessel pericytes and modulates vascular permeability, may result in clinically significant fluid retention, pleural, and pericardial effusions, peripheral edema, and weight gain (34). In contrast, the role of PDGFR $\alpha$  in normal adult physiology appears limited to wound healing (3). Consequently, PDGFR $\alpha$  may be a less toxic and more therapeutically potent target. In a recently completed phase I monotherapy study, no specific adverse events were consistently or conclusively associated with IMC-3G3 (22, 35). Importantly, it has been noted that in cancer cells expressing both PDGF and PDGFR, PDGF forms a complex with PDGFR within the endoplasmic reticulum (36), an intracellular sanctuary site not available to antibody-based therapeutics. However, the PDGF-PDGFR complex generates mitogenic signals only after migration to the cell membrane, where it is accessible to neutralizing antibodies (37).

Partly for reasons described above, clinical trials of PDGFR inhibitors combined with chemotherapy for lung cancer therapy have been negative to date, and some have showed a substantial increase in toxicity (38, 39). However, the results seen with tyrosine kinase inhibitors targeting PDGFR cannot be extrapolated to a highly specific monoclonal antibody such as IMC-3G3. With EGFR inhibitors and antiangiogenic agents, no benefit was seen when tyrosine kinase inhibitors were combined with chemotherapy, but the addition of a monoclonal antibody to chemotherapy improved overall survival (40–44).

The implication that stromal PDGFR targeting could add benefit to NSCLC therapy is substantial. The overwhelming majority of NSCLCs feature stromal PDGFR expression (5, 45, 46). Our findings support the possibility that the therapeutic effects of stromal PDGFR $\alpha$  inhibition may reach beyond the rare cancers sensitive to cancer-cell PDGFR $\alpha$  targeting. In general, stromal targets have a number of favorable properties. They are less prone to mutation than are cancer cell targets.

As shown by the broad clinical use of anti-VEGF antibodies, stromal targeting may be relevant to multiple cancer types. Finally, stromal-directed therapies have been combined effectively and safely with cancer cell-directed treatments, including cytotoxic chemotherapy. As shown in our experiments, for those cancers without tumor cell PDGFR $\alpha$  expression, an anti-PDGFR $\alpha$  antibody may be most effective when combined with conventional chemotherapy or other targeted agents. Accordingly, the results of ongoing phase 2 trials incorporating anti-PDGFR $\alpha$  mAbs into combination therapy for various malignancies are awaited to evaluate this strategy in the clinical setting.

#### Disclosure of Potential Conflicts of Interest

D.E. Gerber and R.A. Brekken receive research funding from ImClone Systems, a wholly owned subsidiary of Eli Lilly and Company, New York, NY. I. Duignan, J. Malaby, T. Bailey, C. Burns, and N. Loizos are employed by ImClone Systems, a wholly owned subsidiary of Eli Lilly and Company, New York, NY.

#### Authors' Contributions

**Conception and design:** D.E. Gerber, Puja Gupta, M. Peyton, R.A. Brekken, N. Loizos

**Development of methodology:** D.E. Gerber, Puja Gupta, M. Peyton, T. Bailey, C. Burns

**Acquisition of data (provided animals, acquired and managed patients, provided facilities, etc.):** D.E. Gerber, Puja Gupta, M.T. Dellinger, J.E. Toombs, M. Peyton, I. Duignan, J. Malaby, C. Burns, N. Loizos

**Analysis and interpretation of data (e.g., statistical analysis, biostatistics, computational analysis):** D.E. Gerber, Puja Gupta, M. Peyton, I. Duignan, J. Malaby, C. Burns, R.A. Brekken, N. Loizos

**Writing, review, and/or revision of the manuscript:** D.E. Gerber, M. Peyton, J. Malaby, C. Burns, R.A. Brekken, N. Loizos

**Administrative, technical, or material support (i.e., reporting or organizing data, constructing databases):** D.E. Gerber, R.A. Brekken  
**Study supervision:** D.E. Gerber, R.A. Brekken, N. Loizos

#### Acknowledgments

The authors acknowledge the assistance of the Biostatistics and Microarray Shared Resources at the Harold C. Simmons Cancer Center, which is supported in part by a National Cancer Institute Cancer Center Support Grant, 1P30 CA142543-01, and the support of Drs. John Minna and Joan Schiller. The authors thank Ilse Valencia for assistance with PDGFR $\alpha$  Western blot analysis and PCR in NSCLC cell lines and immortalized human bronchial epithelial cells. The authors also thank Marie Prewett for help with statistical calculations.

#### Grant Support

Supported by a National Institutes of Health UL1 RR024982 and KL2 RR024938-03 "North and Central Texas Clinical and Translational Science Initiative (NCTCTSI)" grants (D.E. Gerber), a sponsored research agreement from Imclone Systems (D.E. Gerber and R.A. Brekken) and The Effie Marie Cain Scholarship in Angiogenesis Research (R.A. Brekken). P. Gupta was supported by NCI training grant T32CA009640.

The costs of publication of this article were defrayed in part by the payment of page charges. This article must therefore be hereby marked *advertisement* in accordance with 18 U.S.C. Section 1734 solely to indicate this fact.

Received May 1, 2012; revised July 5, 2012; accepted July 30, 2012; published OnlineFirst August 28, 2012.

#### References

- Heldin CH, Ostman A, Ronnstrand L. Signal transduction via platelet-derived growth factor receptors. *Biochim Biophys Acta* 1998;1378: F79–113.
- Soriano P. The PDGF alpha receptor is required for neural crest cell development and for normal patterning of the somites. *Development* 1997;124:2691–700.

3. Ostman A, Heldin CH. Involvement of platelet-derived growth factor in disease: development of specific antagonists. *Adv Cancer Res* 2001;80:1–38.
4. Pietras K, Sjoblom T, Rubin K, Heldin CH, Ostman A. PDGF receptors as cancer drug targets. *Cancer Cell* 2003;3:439–43.
5. Donnem T, Al-Saad S, Al-Shibli K, Andersen S, Busund LT, Bremnes RM. Prognostic impact of platelet-derived growth factors in non-small cell lung cancer tumor and stromal cells. *J Thorac Oncol* 2008;3:963–70.
6. Heinrich MC, Corless CL, Duensing A, McGreevey L, Chen CJ, Joseph N, et al. PDGFRA activating mutations in gastrointestinal stromal tumors. *Science* 2003;299:708–10.
7. Fleming TP, Saxena A, Clark WC, Robertson JT, Oldfield EH, Aaronson SA, et al. Amplification and/or overexpression of platelet-derived growth factor receptors and epidermal growth factor receptor in human glial tumors. *Cancer Res* 1992;52:4550–3.
8. Ramos AH, Dutt A, Mermel C, Perner S, Cho J, Lafargue CJ, et al. Amplification of chromosomal segment 4q12 in non-small cell lung cancer. *Cancer Biol Ther* 2009;8:2042–50.
9. Simon MP, Navarro M, Roux D, Pouyssegur J. Structural and functional analysis of a chimeric protein COL1A1-PDGFB generated by the translocation t(17;22)(q22;q13.1) in Dermatofibrosarcoma protuberans (DF). *Oncogene* 2001;20:2965–75.
10. Cools J, DeAngelo DJ, Gotlib J, Stover EH, Legare RD, Cortes J, et al. A tyrosine kinase created by fusion of the PDGFRA and FIP1L1 genes as a therapeutic target of imatinib in idiopathic hypereosinophilic syndrome. *N Engl J Med* 2003;348:1201–14.
11. McDermott U, Ames RY, Iafrate AJ, Maheswaran S, Stubbs H, Greninger P, et al. Ligand-dependent platelet-derived growth factor receptor (PDGFR)-alpha activation sensitizes rare lung cancer and sarcoma cells to PDGFR kinase inhibitors. *Cancer Res* 2009;69:3937–46.
12. Bauman JE, Eaton KD, Martins RG. Antagonism of platelet-derived growth factor receptor in non small cell lung cancer: rationale and investigations. *Clin Cancer Res* 2007;13:s4632–6.
13. Fukumura D, Xavier R, Sugiura T, Chen Y, Park EC, Lu N, et al. Tumor induction of VEGF promoter activity in stromal cells. *Cell* 1998;94:715–25.
14. Dong J, Grunstein J, Tejada M, Peale F, Frantz G, Liang WC, et al. VEGF-null cells require PDGFR alpha signaling-mediated stromal fibroblast recruitment for tumorigenesis. *EMBO J* 2004;23:2800–10.
15. Loizos N, Xu Y, Huber J, Liu M, Lu D, Finnerty B, et al. Targeting the platelet-derived growth factor receptor alpha with a neutralizing human monoclonal antibody inhibits the growth of tumor xenografts: implications as a potential therapeutic target. *Mol Cancer Ther* 2005;4:369–79.
16. Gazdar AF, Girard L, Lockwood WW, Lam WL, Minna JD. Lung cancer cell lines as tools for biomedical discovery and research. *J Natl Cancer Inst* 2010;102:1310–21.
17. Karlen Y, McNair A, Perseguers S, Mazza C, Mermod N. Statistical significance of quantitative PCR. *BMC Bioinform* 2007;8:131.
18. de Haard HJ, van Neer N, Reurs A, Hufton SE, Roovers RC, Henderikx P, et al. A large non-immunized human Fab fragment phage library that permits rapid isolation and kinetic analysis of high affinity antibodies. *J Biol Chem* 1999;274:18218–30.
19. Lu D, Jimenez X, Zhang H, Bohlen P, Witte L, Zhu Z. Selection of high affinity human neutralizing antibodies to VEGFR2 from a large antibody phage display library for antiangiogenesis therapy. *Int J Cancer* 2002;97:393–9.
20. Burtrum D, Zhu Z, Lu D, Anderson DM, Prewett M, Pereira DS, et al. A fully human monoclonal antibody to the insulin-like growth factor I receptor blocks ligand-dependent signaling and inhibits human tumor growth *in vivo*. *Cancer Res* 2003;63:8912–21.
21. Dineen SP, Roland CL, Greer R, Carbon JG, Toombs JE, Gupta P, et al. Smac mimetic increases chemotherapy response and improves survival in mice with pancreatic cancer. *Cancer Res* 2010;70:2852–61.
22. Youssoufian H, Amato RJ, Sweeney C, Chiorean EG, Fox F, Katz T, et al. Phase 1 study of IMC-3G3, an IgG1 monoclonal antibody targeting PFGDRa in patients with advanced solid malignancies. *J Clin Oncol* 2008;26 (May 20 suppl). Abstract 14617.
23. Peres R, Betsholtz C, Westermark B, Heldin CH. Frequent expression of growth factors for mesenchymal cells in human mammary carcinoma cell lines. *Cancer Res* 1987;47:3425–9.
24. Vignaud JM, Marie B, Klein N, Plenat F, Pech M, Borrelly J, et al. The role of platelet-derived growth factor production by tumor-associated macrophages in tumor stroma formation in lung cancer. *Cancer Res* 1994;54:5455–63.
25. Ichihara E, Ohashi K, Takigawa N, Osawa M, Ogino A, Tanimoto M, et al. Effects of vandetanib on lung adenocarcinoma cells harboring epidermal growth factor receptor T790M mutation *in vivo*. *Cancer Res* 2009;69:5091–8.
26. Kitadai Y, Sasaki T, Kuwai T, Nakamura T, Bucana CD, Fidler IJ. Targeting the expression of platelet-derived growth factor receptor by reactive stroma inhibits growth and metastasis of human colon carcinoma. *Am J Pathol* 2006;169:2054–65.
27. Yu J, Liu XW, Kim HR. Platelet-derived growth factor (PDGF) receptor-alpha-activated c-Jun NH2-terminal kinase-1 is critical for PDGF-induced p21WAF1/CIP1 promoter activity independent of p53. *J Biol Chem* 2003;278:49582–8.
28. Sullivan LA, Carbon JG, Roland CL, Toombs JE, Nyquist-Andersen M, Kavlie A, et al. r84, a novel therapeutic antibody against mouse and human VEGF with potent anti-tumor activity and limited toxicity induction. *PLoS One* 2010;5:e12031.
29. Pietras K, Ostman A, Sjoquist M, Buchdunger E, Reed RK, Heldin CH, et al. Inhibition of platelet-derived growth factor receptors reduces interstitial hypertension and increases transcapillary transport in tumors. *Cancer Res* 2001;61:2929–34.
30. Pietras K, Rubin K, Sjoblom T, Buchdunger E, Sjoquist M, Heldin CH, et al. Inhibition of PDGF receptor signaling in tumor stroma enhances antitumor effect of chemotherapy. *Cancer Res* 2002;62:5476–84.
31. Shao ZM, Nguyen M, Barsky SH. Human breast carcinoma desmoplasia is PDGF initiated. *Oncogene* 2000;19:4337–45.
32. Alvares O, Klebe R, Grant G, Cochran DL. Growth factor effects on the expression of collagenase and TIMP-1 in periodontal ligament cells. *J Periodontol* 1995;66:552–8.
33. Forsberg K, Valyi-Nagy I, Heldin CH, Herlyn M, Westermark B. Platelet-derived growth factor (PDGF) in oncogenesis: development of a vascular connective tissue stroma in xenotransplanted human melanoma producing PDGF-BB. *Proc Natl Acad Sci U S A* 1993;90:393–7.
34. Mauro MJ, Deininger MW. Management of drug toxicities in chronic myeloid leukaemia. *Best Pract Res Clin Haematol* 2009;22:409–29.
35. Shah GD, Loizos N, Youssoufian H, Schwartz JD, Rowinsky EK. Rationale for the development of IMC-3G3, a fully human immunoglobulin G subclass 1 monoclonal antibody targeting the platelet-derived growth factor receptor alpha. *Cancer* 2010;116:1018–26.
36. Keating MT, Williams LT. Autocrine stimulation of intracellular PDGF receptors in v-sis-transformed cells. *Science* 1988;239:914–6.
37. Fleming TP, Matsui T, Molloy CJ, Robbins KC, Aaronson SA. Autocrine mechanism for v-sis transformation requires cell surface localization of internally activated growth factor receptors. *Proc Natl Acad Sci U S A* 1989;86:8063–7.
38. Tsao AS, Liu S, Fujimoto J, Wistuba II, Lee JJ, Marom EM, et al. Phase II trials of imatinib mesylate and docetaxel in patients with metastatic non-small cell lung cancer and head and neck squamous cell carcinoma. *J Thorac Oncol* 2011;6:2104–11.
39. Huang CH, Williamson SK, Van Veldhuizen PJ, Hsueh CT, Allen A, Tawfik O, et al. Potential role of platelet-derived growth factor receptor inhibition using imatinib in combination with docetaxel in the treatment of recurrent non-small cell lung cancer. *J Thorac Oncol* 2011;6:372–7.
40. Herbst RS, Prager D, Hermann R, Fehrenbacher L, Johnson BE, Sandler A, et al. TRIBUTE: a phase III trial of erlotinib hydrochloride (OSI-774) combined with carboplatin and paclitaxel chemotherapy in advanced non-small-cell lung cancer. *J Clin Oncol* 2005;23:5892–9.
41. Giaccone G, Herbst RS, Manegold C, Scagliotti G, Rosell R, Miller V, et al. Gefitinib in combination with gemcitabine and cisplatin in advanced non-small-cell lung cancer: a phase III trial-INTACT 1. *J Clin Oncol* 2004;22:777–84.
42. Scagliotti G, Von Pawel J, Reck M, Cupit L, Cihon F, DiMatteo J, et al. Sorefenib plus carboplatin/paclitaxel in chemo-naive patients with

- stage IIIB-IV non-small cell lung cancer (NSCLC): interim analysis results from the phase III, randomized controlled ESCAPE (Evaluation of Sorafenib, Carboplatin, and Paclitaxel Efficacy in NSCLC) Trial, *J Thorac Oncol* 2008;3(4, Suppl. 1): Late Breaking Abstract 275, page S97.
43. Pirker R, Pereira JR, Szczesna A, von Pawel J, Krzakowski M, Ramlau R, et al. Cetuximab plus chemotherapy in patients with advanced non-small-cell lung cancer (FLEX): an open-label randomised phase III trial. *Lancet* 2009;373:1525–31.
44. Sandler A, Gray R, Perry MC, Brahmer J, Schiller JH, Dowlati A, et al. Paclitaxel-carboplatin alone or with bevacizumab for non-small-cell lung cancer. *N Engl J Med* 2006;355:2542–50.
45. Kawai T, Hiroi S, Torikata C. Expression in lung carcinomas of platelet-derived growth factor and its receptors. *Lab Invest* 1997;77:431–6.
46. Donnem T, Al-Shibli K, Al-Saad S, Busund LT, Bremnes RM. Prognostic impact of fibroblast growth factor 2 in non-small cell lung cancer: coexpression with VEGFR-3 and PDGF-B predicts poor survival. *J Thorac Oncol* 2009;4:578–85.

# Molecular Cancer Therapeutics

## Stromal Platelet-Derived Growth Factor Receptor $\alpha$ (PDGFR $\alpha$ ) Provides a Therapeutic Target Independent of Tumor Cell PDGFR $\alpha$ Expression in Lung Cancer Xenografts

David E. Gerber, Puja Gupta, Michael T. Dellinger, et al.

*Mol Cancer Ther* 2012;11:2473-2482. Published OnlineFirst August 28, 2012.

**Updated version** Access the most recent version of this article at:  
[doi:10.1158/1535-7163.MCT-12-0431](https://doi.org/10.1158/1535-7163.MCT-12-0431)

**Supplementary Material** Access the most recent supplemental material at:  
<http://mct.aacrjournals.org/content/suppl/2012/08/28/1535-7163.MCT-12-0431.DC1>

**Cited articles** This article cites 44 articles, 20 of which you can access for free at:  
<http://mct.aacrjournals.org/content/11/11/2473.full#ref-list-1>

**Citing articles** This article has been cited by 4 HighWire-hosted articles. Access the articles at:  
<http://mct.aacrjournals.org/content/11/11/2473.full#related-urls>

**E-mail alerts** [Sign up to receive free email-alerts](#) related to this article or journal.

**Reprints and Subscriptions** To order reprints of this article or to subscribe to the journal, contact the AACR Publications Department at [pubs@aacr.org](mailto:pubs@aacr.org).

**Permissions** To request permission to re-use all or part of this article, use this link  
<http://mct.aacrjournals.org/content/11/11/2473>.  
Click on "Request Permissions" which will take you to the Copyright Clearance Center's (CCC) Rightslink site.